**Electronic Supplementary Information**

Interface Suppressed High-Quality Symmetrical Bifacial Flexible CZTSe Solar Cells through a Green Electrodeposition Process

Jingling Liu,[a] Hang Cai,[a] Xinyu Wu,[a] Sheng Liu,[a] Ying Xue,[a] Xinsheng Liu,[a] Ke Cheng*[a] and Zuliang Du*[a]


[a] Key Laboratory for Special Functional Materials of Ministry of Education, National & Local Joint Engineering Research Center for High-efficiency Display and Lighting Technology, School of Materials Science and Engineering, and Collaborative Innovation Center of Nano Functional Materials and Applications, Henan University, Kaifeng 475004, China
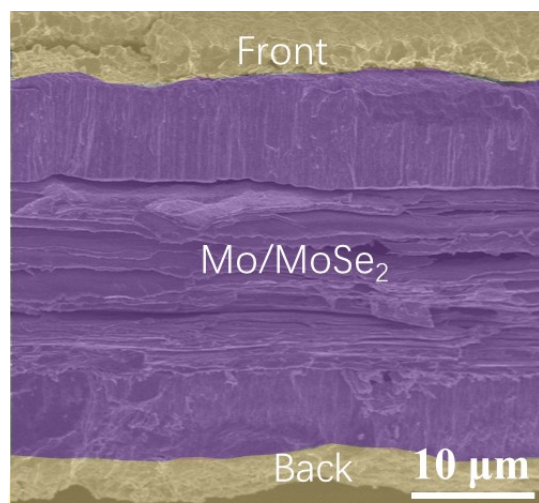
Corresponding Author
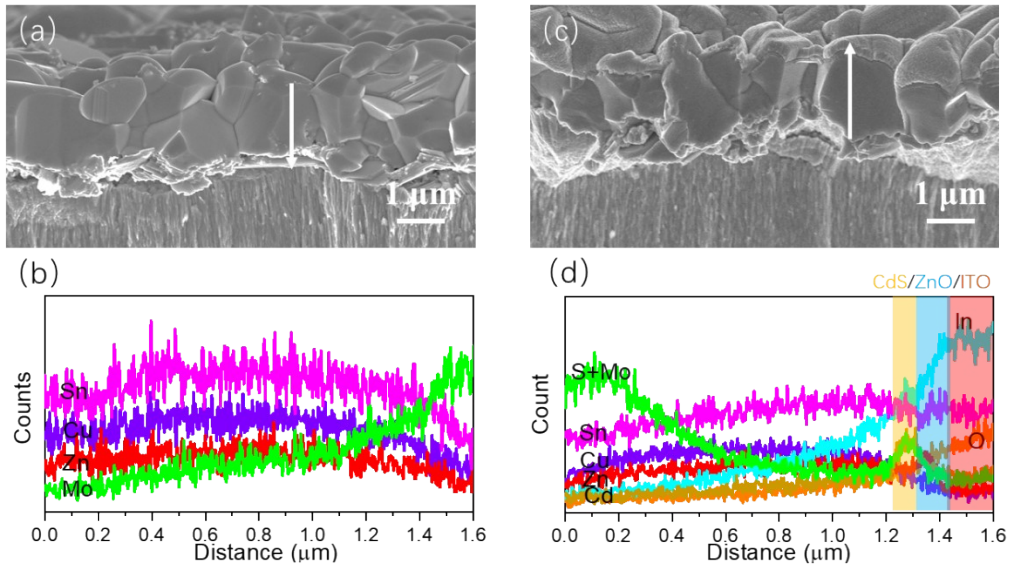
*zld@henu.edu.cn, ck@henu.edu.cn
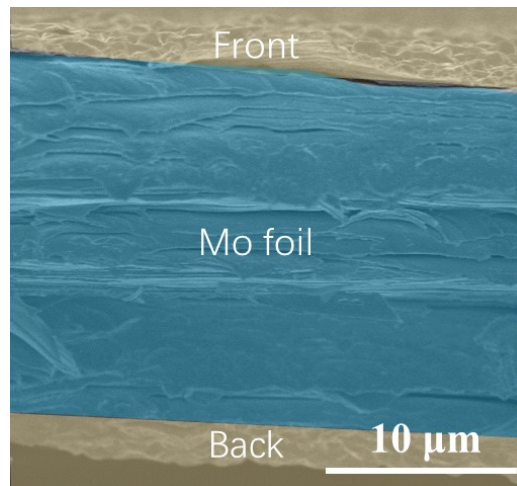
Figure S1. Cross-section SEM image of bifacial flexible Cu/Sn/Zn preformed layers.
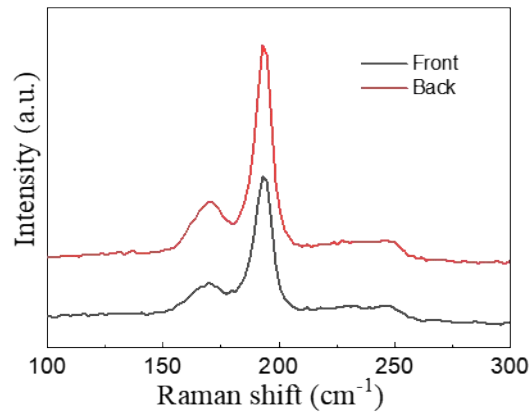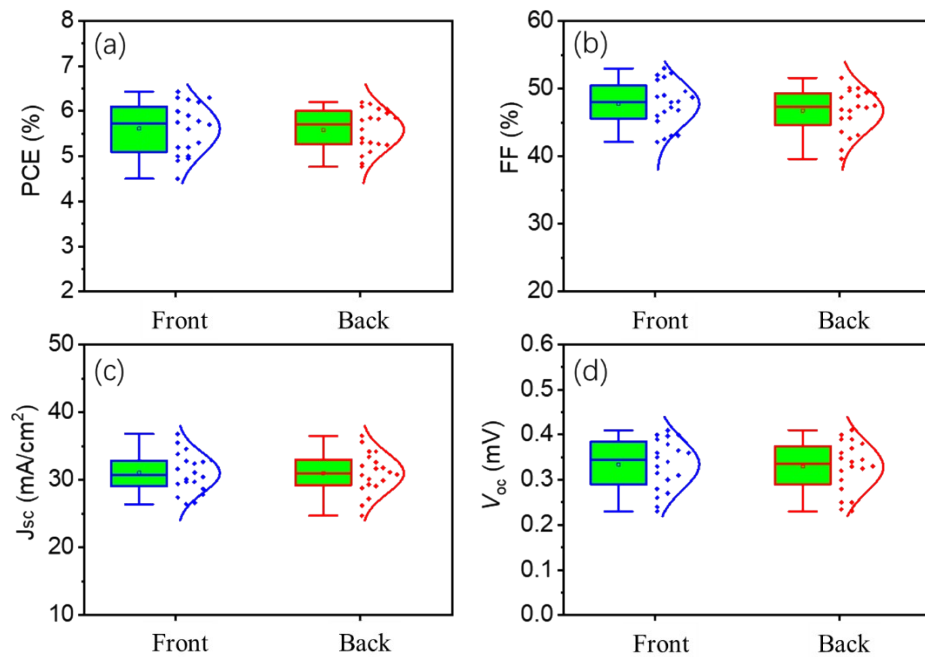

**Figure S2.** Raman spectra for bifacial flexible CZTSe thin films.

Figure S3. Cross-section SEM image of bifacial flexible CZTSe devices.

Figure S4. (a and b) cross-sectional SEM images and EDS line scanning profiles along the white lines for the absorber layer and devices, respectively (a and b for the absorber layer; c and d for the device).
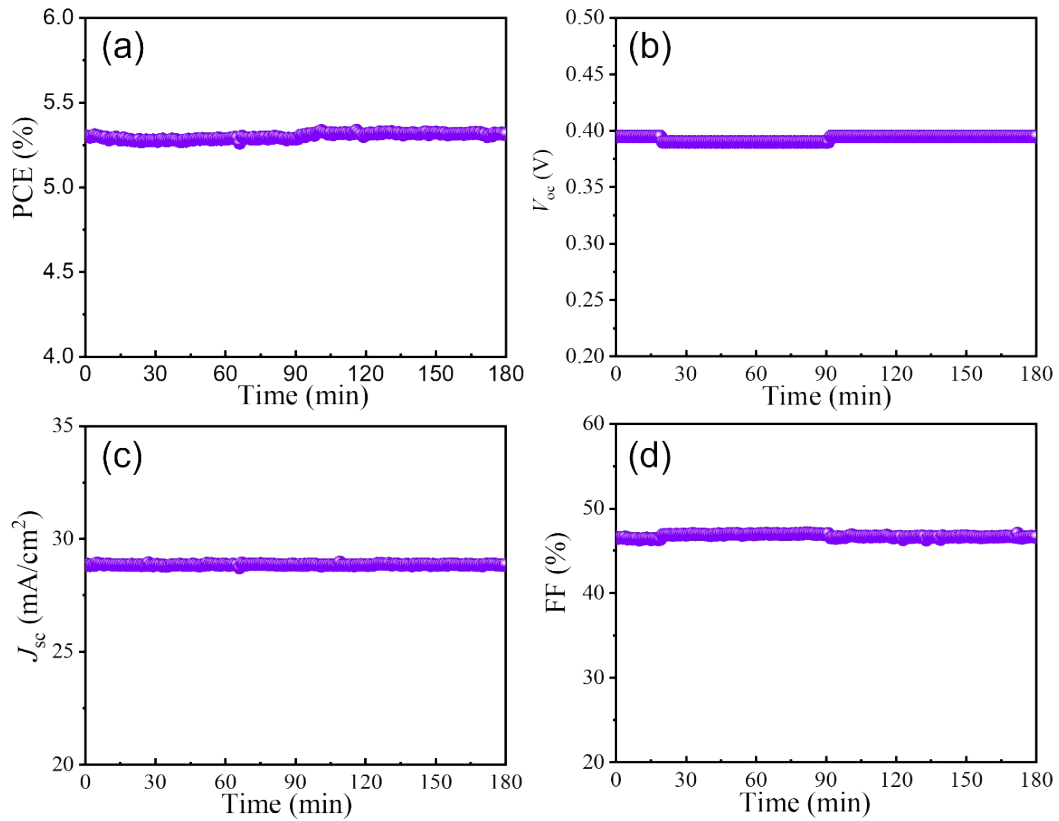

Figure S5. Statistical distribution of PCE, FF, J_{sc} and V_{oc} for bifacial flexible CZTSe solar cells.
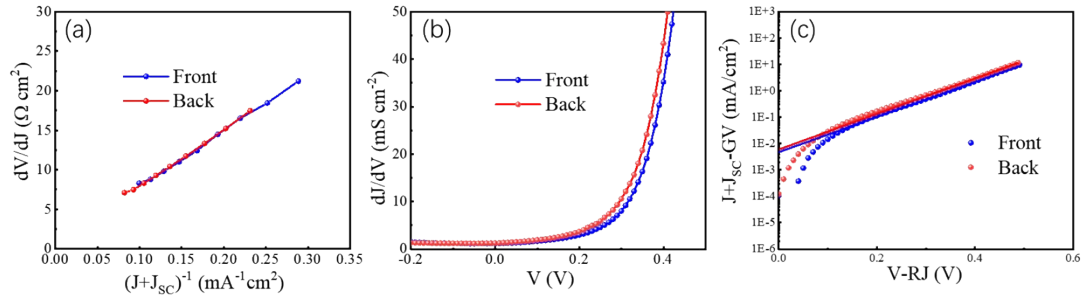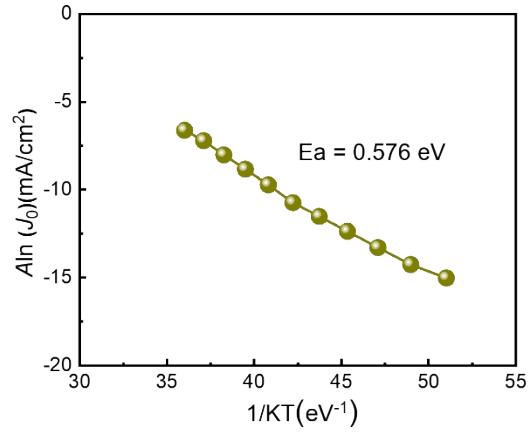
Figure S6. (a) The Plots of dV/dJ versus $(J+J_{sc})^{-1}$, dJ/dV vs V, and $J+J_{sc}$-GV vs V-R$_s J$, respectively, for the bifacial flexible CZTSe solar cells extracted from dark J-V.

Figure S7. (a-d) The variations of PCE, V_{oc}, J_{sc}, and FF for continuously irradiation for 3h.

Figure S8. $A \ln(J_0)$ vs. $1/KT$ plot of CZTSe device extracted from J-V-T curve in Figure 5f.